

Understanding the sub-seasonal variation in the wintertime AO spatial pattern from the viewpoint of El Niño-Southern Oscillation

Sugiong Hu¹ · Wenjun Zhang¹ · Feng Jiang¹ · Fei-Fei Jin²

Received: 27 March 2022 / Accepted: 3 October 2022 © The Author(s), under exclusive licence to Springer-Verlag GmbH Germany, part of Springer Nature 2022

Abstract

The wintertime Arctic Oscillation (AO) manifests a high degree of uncertainty in its spatial structure, which was suggested to be associated with some other extratropical atmospheric variabilities (e.g., the Aleutian-Icelandic Low seesaw and the stratospheric polar vortex). Based on reanalysis and model simulation data in 1950–2019, the present work investigates the possible effects of El Niño-Southern Oscillation (ENSO) on the AO spatial structure. It is found that there exist obvious differences in AO structure between early (November–December) and late (January–February) winter. In early winter, the AO is manifested by its traditional pattern with three action centers, one of which is over the Arctic and the other two are with the opposite sign over the North Atlantic and North Pacific. However, the AO pattern in late winter changes remarkably, resembling a regional North Atlantic Oscillation (NAO) pattern with the absence of its significant Pacific center. The noteworthy sub-seasonal variation in the AO spatial pattern can be largely ascribed to the observed fact that ENSO atmospheric teleconnections to the Northern Hemisphere are significantly enhanced in late winter compared with early winter. The enhanced ENSO-associated teleconnection during late winter can significantly weaken the teleconnectivity of the Arctic center with the Pacific center, resulting in the absence of the AO's significant Pacific center. The understanding of ENSO impacts on the AO structure has some significance for the AO-associated climate prediction around the North Pacific region.

Keywords AO structure · ENSO · Early winter · Late winter

1 Introduction

The Arctic Oscillation (AO) is usually represented by the first Empirical Orthogonal Function (EOF) mode of the sea level pressure (SLP) anomalies over 20° N–90° N (Thompson and Wallace 1998). It manifests a meridional seesaw in the circulation field between the polar and mid-latitude regions of the Northern Hemisphere. The positive AO phase is characterized by negative SLP anomalies over the Arctic paired with positive SLP anomalies over the North Atlantic and North Pacific, and vice versa. It is now well

established from a variety of studies, that the AO has considerable effects on the global weather and climate anomalies, such as air temperature, precipitation, tropical cyclone, etc. (e.g., Wang 2005; Choi and Byun 2010; Mao et al. 2011). Some studies also found that spring AO can exert a marked impact on the succedent winter El Niño-Southern Oscillation (ENSO) (Nakamura et al. 2006; Chen et al. 2014, 2015).

Since the AO pattern is determined based on statistical analyses, the question naturally arises whether the AO can be interpreted as a physical/dynamical mode of climate variability. Through examining the teleconnectivity among the three centers of the AO, Deser (2000) found that only two centers are strongly related (i.e., Arctic and North Atlantic centers), whereas the North Pacific center is uncorrelated with the other two. One further study pointed out that an EOF analysis could produce apparent modes different from the preset modes by designing artificial orthogonal vectors (Dommenget and Latif 2002). Since the North Atlantic Oscillation (NAO) pattern can be consistently identified in a variety of physical variable fields, it is generally considered to be a more robust physical mode than the AO pattern

Published online: 18 October 2022



Wenjun Zhang zhangwj@nuist.edu.cn

CIC-FEMD/ILCEC, Key Laboratory of Meteorological Disaster of Ministry of Education (KLME), College of Atmospheric Sciences, Nanjing University of Information Science and Technology, Nanjing 210044, China

Department of Meteorology, School of Ocean and Earth Science and Technology, University of Hawai'i at Manoa, Honolulu, HI 96822, USA

(Ambaum et al. 2001; Feldstein and Franzke 2006). Contrastingly, Christiansen (2002) applied a rotated EOF analysis in the middle troposphere circulation field and argued that the AO can be interpreted as a physical mode rather than a product of statistical analysis. This is consistent with Wallace and Thompson (2002), where the AO could be identified as a reliable physical mode and the NAO is thus viewed as the North Atlantic component of the AO. They demonstrated that other extratropical atmospheric variability may mask the AO signal at mid-latitudes. Once the second EOF mode of the SLP is linearly removed from the original SLP field, the two centers of the AO at mid-latitudes become more strongly correlated.

Despite that debates continue on the true nature of the AO (e.g., Mori et al. 2006; Itoh et al. 2007; Itoh 2008; Cheng and Tan 2019), considerable literature has grown up around the uncertainty of the wintertime AO pattern as well as its physical mechanism. One study suggested that an Aleutian-Icelandic Low seesaw (AIS) can affect the spatial pattern of the late winter AO by changing inter-basin teleconnectivity (Honda 2001; Shi and Nakamura 2014). The Pacific center of AO is present during an active AIS period, while it disappears during an inactive AIS period. Similarly, the stratospheric process is also argued to exert impacts on the AO spatial pattern (Castanheira and Graf 2003; Cheng and Tan 2019; Gong et al. 2019b). The North Pacific center related to the AO is strong (weak) for the strong (weak) stratospheric polar vortex events.

The existing evidence shows that the complexity in the AO spatial pattern largely originates from the high degree of uncertainty of its North Pacific center (Honda 2001; Shi and Nakamura 2014; Gong et al. 2018; Cheng and Tan 2019). As the predominant interannual air-sea coupled mode in the equatorial Pacific (e.g., Bjerknes 1967; Neelin et al. 1998; Philander 2018), ENSO can significantly affect climate variability over the North Pacific via the Pacific North American (PNA) pattern (e.g., Horel and Wallace 1981; Livezey and Mo 1987; Wang and Fu 2000). It is compelling to hypothesize that the ENSO should have some influence on the AO spatial structure by exciting extratropical teleconnection patterns. If ENSO does affect the spatial structure of AO, it would have some implications for the AO-related regional climate prediction given distinct regional climate impacts for the different AO structures (Gong et al. 2018, 2019b; Cheng and Tan 2019).

In this work, we investigate the possible ENSO effects on the AO spatial structure variations and the associated physical mechanisms. Since the extratropical atmospheric responses to ENSO are very different between early (November–December) and late winter (January–February) (e.g., Livezey et al. 1997; Moron and Gouirand 2003; Bladé et al. 2008; Kim et al. 2018), the AO structures in early and late winter are here separated to emphasize potentially different

ENSO impacts. Our work demonstrates that obviously different AO structures are detected over the North Pacific in early and late winter, and the remarkable sub-seasonal change can be largely ascribed to the enhancement of ENSO teleconnection to the extratropical atmosphere. In the rest of this paper, Sect. 2 introduces the data and methods. Section 3 presents obvious differences in the AO structure in early and late winter. Section 4 investigates ENSO impacts on the spatial pattern of the winter AO. Furthermore, possible mechanisms are addressed in Sect. 5. Finally, we summarize the main conclusions and offer related discussions in Sect. 6.

2 Data and methodology

The datasets employed in this work are as follows: (1) monthly and daily mean atmospheric circulation data obtained from the National Centers for Environmental Prediction/National Center for Atmospheric Research (NCEP/ NCAR) reanalysis data (Kalnay et al. 1996). The data has a horizontal resolution of $2.5^{\circ} \times 2.5^{\circ}$ and a vertical resolution of 17 levels, including SLP, 500hPa geopotential height (Z500), and 200hPa horizontal wind. (2) monthly mean sea surface temperature (SST) data on a $1^{\circ} \times 1^{\circ}$ grid derived from the Met Office Hadley Centre (Rayner et al. 2003). The datasets span the period 1950–2019, and anomalies are obtained by removing the monthly mean of 1950-2019. In addition, the Atmospheric Model Inter-comparison Project (AMIP)-style simulations of MRI-ESM-2-0 model from 1979 to 2014 are used to verify the ENSO impacts on the AO structure (Eyring et al. 2016). Descriptions of this model are given by Yukimoto et al. (2019). Here, all three ensemble members of the model are utilized. All of the model data are bi-linearly interpolated into a $2.5^{\circ} \times 2.5^{\circ}$ horizontal grid for comparison with the reanalysis data.

Following previous studies (Thompson and Wallace 1998, 2001), the AO index is defined as the corresponding time series of the first EOF mode of the SLP variability in the region north of 20° N. We employ the covariance matrix for the EOF analysis. The SLP data are weighted by the square root of the cosine of latitude to guarantee equal-area weighting for the covariance matrix. AO events are identified based on the definition in Cheng and Tan (2019), with a threshold of \pm 0.5 standard deviation here. Rossby wave source (RWS) magnitude is employed to analyze the ENSO atmospheric teleconnections to the North Pacific (Sardeshmukh and Hoskins 1988). Three indices are defined to describe the intensity of the three AO centers. Specifically, the Arctic center index is defined as the standardized area-averaged SLP anomalies over the Arctic (60° W-90° E, 60° N-80° N). The Atlantic center index is measured as the standardized area-averaged SLP anomalies



over the North Atlantic (70° W– 40° E, 20° N– 50° N). The Pacific center index is calculated by the standardized areaaveraged SLP anomalies over the North Pacific (120° W–0°, 20° N-50° N). The choice of these domains is based on the regressed SLP anomalies on the early winter AO index. The boreal winter is divided into early winter (ND, November-December) and late winter (JF, January-February) in this study. For convenience, we here define the difference between the Atlantic center index and the Arctic center index as the NAO index. The Niño3.4 index (SST anomalies averaged over 5° S-5° N and 120° W-170° W) is utilized as a representation of ENSO variability. 25 El Niño and 22 La Niña winters in the period of 1950–2019 are identified by Climate Prediction Center (CPC) based on a threshold of ± 0.5 standard deviation of the Niño3.4 index (Table 1). The year listed in Table 1 corresponds to year(0)/year(1), where 0 and 1 stand for the developing years of ENSO events and the following years, respectively. The statistical significance is performed by the two-tailed Student's t-test. The Fisher r-to-z transformation is employed to analyze the difference between two correlation coefficients (Fisher 1915, 1921). Furthermore, the rotated EOF analysis method is utilized to identify the robustness of the results (Kaiser 1958). This rotation is based on the first 10 EOFs, which explain more than 80% of its variance. It shows that the qualitative conclusions remain the same (figures not shown). In this study, we also use the bootstrapping method to verify the AO spatial pattern during normal and ENSO years (Deser et al. 2017).

3 The difference in the AO structure in early and late winter

Figures 1a and b show the EOF1 modes of the SLP anomalies in early and late winter, which explain 21.2% and 28.2% of the total variance, respectively. In early winter, the spatial

Table 1 El Niño and La Niña winters

El Niño 1951/1952, 1953/1954, 1957/1958, 1958/1959, 1963/1964, 1965/1966, 1968/1969, 1969/1970, 1972/1973, 1976/1977, 1977/1978, 1979/1980, 1982/1983, 1986/1987, 1987/1988, 1991/1992, 1994/1995, 1997/1998, 2002/2003, 2004/2005, 2006/2007, 2009/2010, 2014/2015, 2015/2016, 2018/2019

La Niña 1954/1955, 1955/1956, 1964/1965, 1970/1971, 1971/1972, 1973/1974, 1974/1975, 1975/1976, 1983/1984, 1984/1985, 1988/1989, 1995/1996, 1998/1999, 1999/2000, 2000/2001, 2005/2006, 2007/2008, 2008/2009, 2010/2011, 2011/2012, 2016/2017, 2017/2018

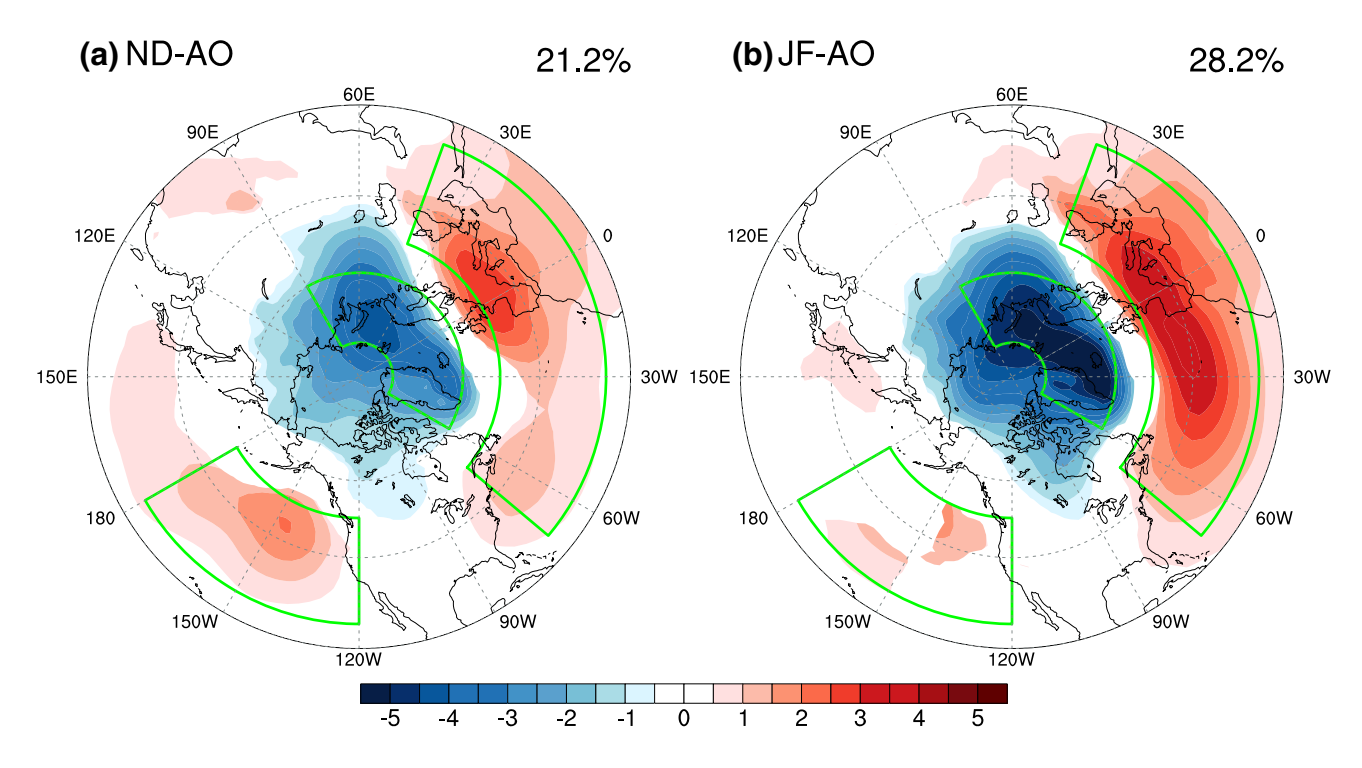


Fig. 1 a The early winter AO pattern represented by the regressed anomalous pattern of SLP (hPa) on the early winter AO index. b The late winter AO pattern represented by the regressed anomalous pat-

tern of SLP (hPa) on the late winter AO index. The SLP anomalies significant above the 95% confidence levels are shaded. The green boxes in **a** and **b** are the domains used to define three action centers



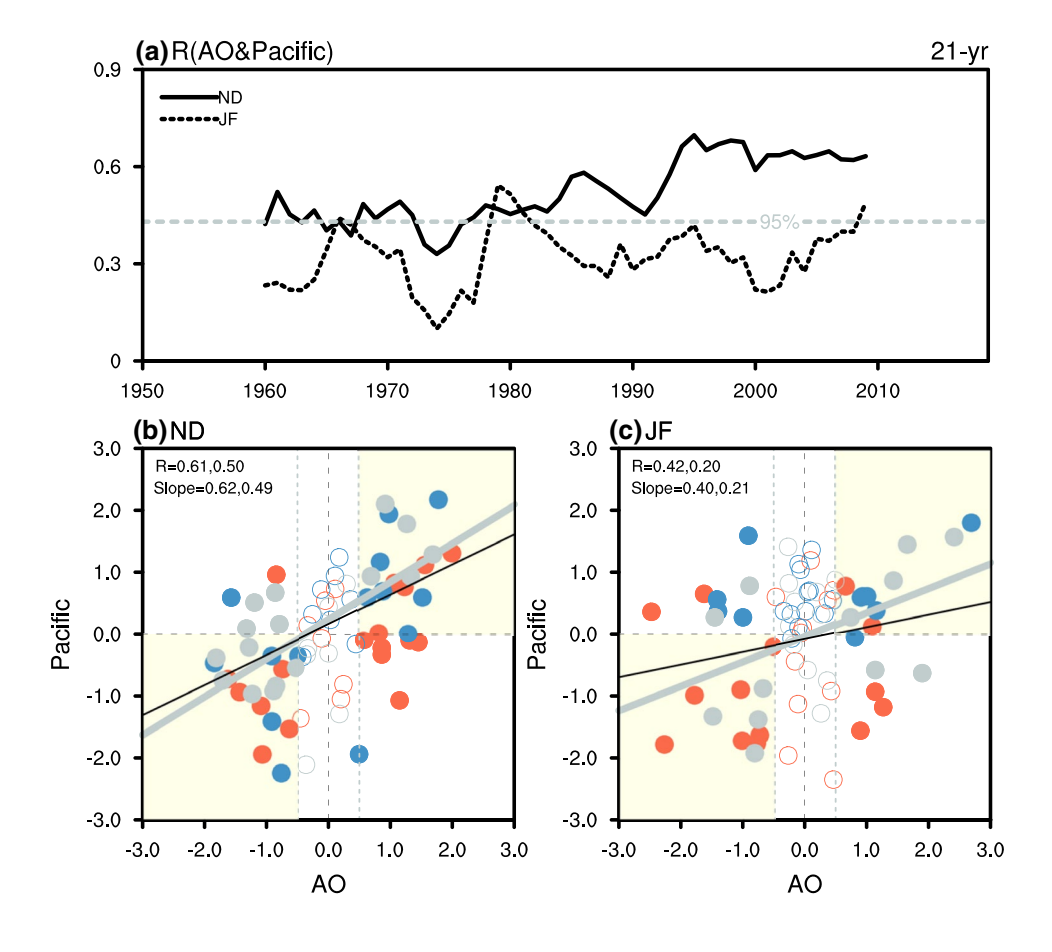
structure of the EOF1 mode manifests as a traditional AO pattern, distinguished by an SLP seesaw with the negative SLP anomalies over the Arctic and positive SLP anomalies at the two mid-latitude centers (Fig. 1a). The spatial pattern of the AO in late winter differs largely from that in early winter. As shown in Fig. 1b, no statistically significant large-scale circulation anomalies can be detected in the North Pacific region. The AO only consists of two action centers: one over the Arctic and the other over the North Atlantic, which is featured with a less-annular spatial structure compared with that in early winter. It is also observed that the SLP anomalies in the Arctic and Atlantic regions for late winter are stronger than that in early winter, which has been mentioned by Thompson and Wallace (2000).

The correlation coefficients of the AO with NAO indices are 0.92 in early winter and 0.97 in late winter. This suggests the Arctic and Atlantic centers of the AO are stationary, in accordance with previous investigations (Deser 2000; Gong et al. 2018). A statistically significant relationship can be found between the early winter AO index and its Pacific center (R = 0.52). However, the correlation becomes weak (R = 0.28) in late winter, accompanied by the absence of the AO's significant Pacific center in Fig. 1b. The difference between the two correlation coefficients is statistically significant at the 90% confidence level, further confirming

a contrast of the AO spatial patterns in the North Pacific region between early and late winter (Figs.1a, b). The results are further evidenced by a 21-year running correlation of the AO with its Pacific center. As displayed in Fig. 2a, the early winter AO and its Pacific center are significantly correlated in almost the whole study period based on the 95% confidence level with an obvious rise since 1992, while nearly no significant correlation can be detected in late winter.

To understand the sub-seasonal change of the AO pattern over the North Pacific, Fig. 2b and c show the scatterplots of the AO and its Pacific center for early and late winter, respectively. In early winter, there are 47 AO years detected (i.e., the year with the AO index exceed $ing \pm 0.5$ standard deviation). Among them, the AO indices of 35 years (74%) have the same signs as the Pacific center indices, confirming the results in Figs. 1 and 2a. Moreover, the AO and its Pacific center have statistically significant correlations both in normal years (R = 0.61)and ENSO years (R = 0.50) (Fig. 2b). No statistically significant difference is found between the two correlation coefficients, manifesting that ENSO has little effect on the early winter AO structure. In contrast, the Pacific center exhibits a high degree of uncertainty in its relationship with the AO during late winter (Fig. 2c). 21 of 35 AO years (60%) have the same signs for the AO index

Fig. 2 a The 21-year running correlations of the AO index with Pacific center index for early (black solid line) and late winter (black dashed line). The gray dashed line represents the 95% confidence level. b The scatter plot of the early winter AO index and Pacific center index for the ENSO warm (red). cold (blue), and neutral (gray) events. The dots with the AO index exceeding ± 0.5 standard deviation are marked as the filled circles (i.e., AO years). The linear fits for normal years (gray line) and ENSO years (black line) are presented with respective correlation coefficients (R) and slopes, and these fits are based on the filled circles. c Same as b, but for the late winter. The yellow shading area denotes that the AO and its Pacific center indices are of the same sign

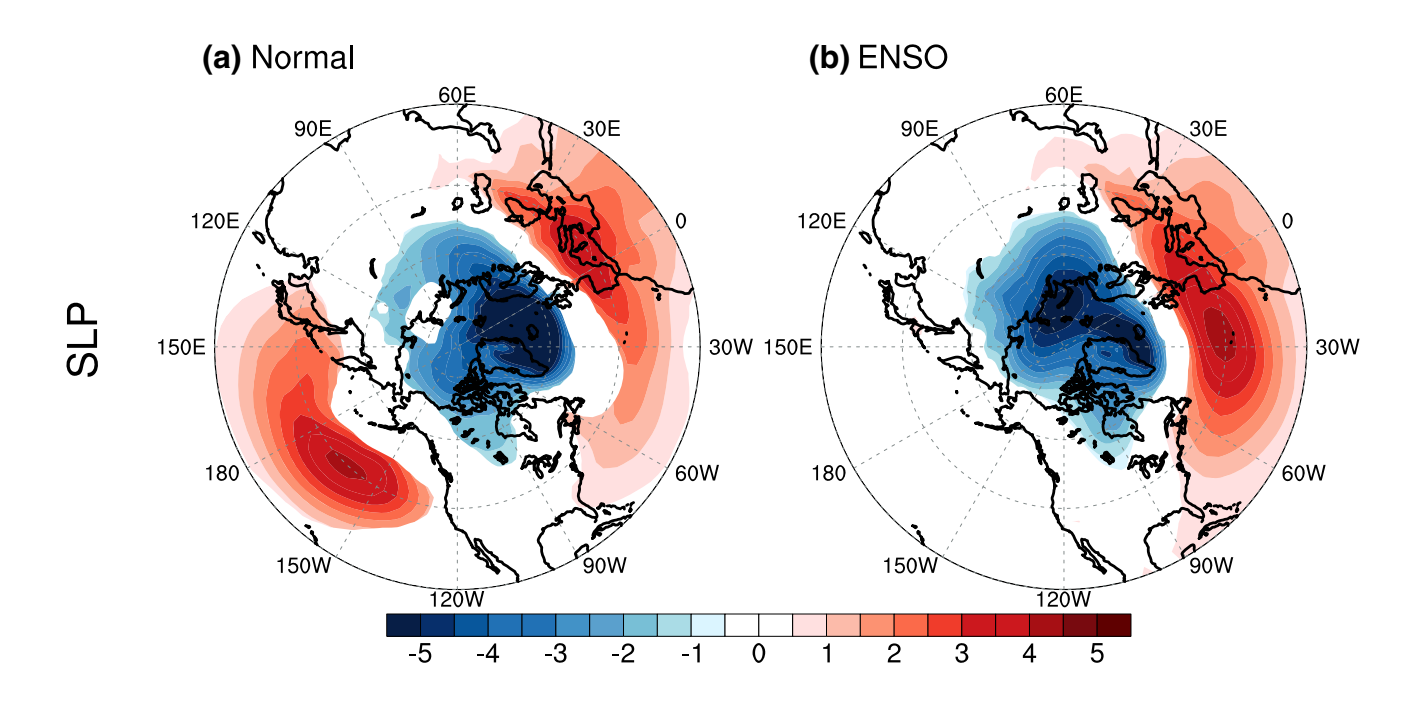




and its Pacific center index. Interestingly, the AO index is statistically significantly related to its Pacific center index (R=0.42) for normal years and while a nonsignificant correlation (R=0.20) is observed for ENSO years.

4 ENSO impacts on the winter AO spatial structure

The above observation leads us to hypothesize that ENSO should affect the AO spatial structure during late winter. To inspect possible ENSO impacts, we in Fig. 3 display the anomalies of SLP and 500 hPa geopotential height regressed



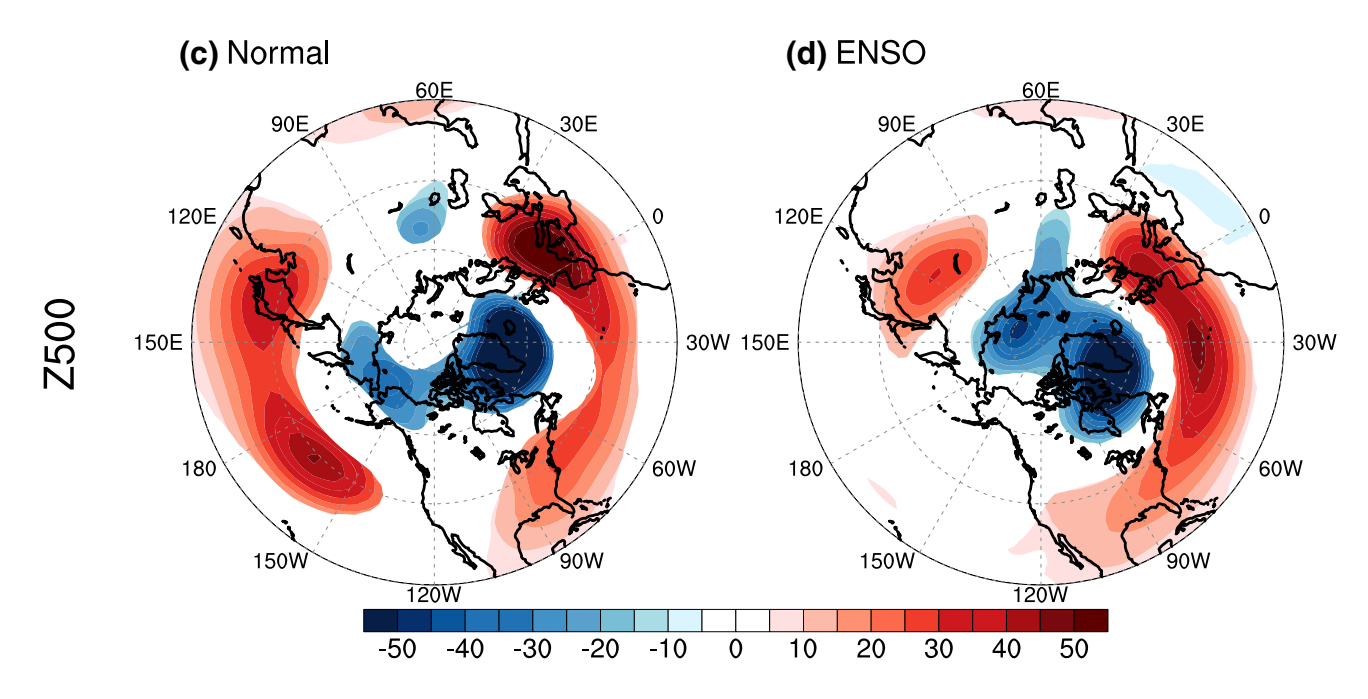


Fig. 3 a The late winter AO pattern for normal years represented by the regressed anomalous pattern of SLP (hPa) on the late winter AO index during normal years of 1950–2019. **b** Same as **a**, but for the

ENSO years. **c** Same as **a**, but for the Z500 anomalies (m). **d** Same as **b**, but for the Z500 anomalies (m). Shading represents those anomalies significant above the 95% confidence levels

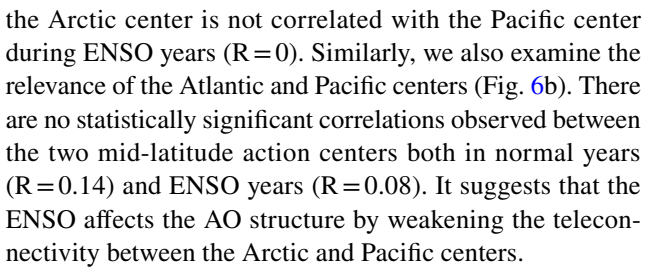


onto the late winter AO index in normal and ENSO years. The AO-related SLP pattern in normal years is composed of three action centers, one of which is over the Arctic and the other two are over the North Atlantic and North Pacific with opposite signs, exhibiting an obvious annularity like an AO traditional pattern (Fig. 3a). Contrastingly, no statistically significant SLP anomalies can be detected over the North Pacific for ENSO years (Fig. 3b). The dipolar seesaw pattern in the SLP field over the Arctic and North Atlantic resembles a regional NAO pattern. The above differences can also be observed in the 500 hPa geopotential height field (Figs. 3c, d), exhibiting significantly positive anomalies in the North Pacific region for normal years, but not for ENSO years. We also generated 1000 bootstrapped samples to verify the late winter AO spatial pattern during normal and ENSO years. The averaged bootstrapping regression coefficients bears a close resemblance to that in Fig. 3. Furthermore, the interquartile ranges of the AO's North Pacific center from these samples for the normal and ENSO years do not overlap, which indicates the robustness of ENSO impact on the AO spatial pattern (figures not shown). It is shown that the ENSO has significant effects on the late winter AO spatial structure, distinctly different from that in early winter. In early winter, the AO is manifested by its traditional pattern with three action centers both in normal years (Fig. 4a, c) and ENSO years (Fig. 4b, d).

We also inspect whether the absence of the significant Pacific center in the late winter AO spatial pattern can be detected both in the ENSO warm and cold phases. For El Niño years, significantly negative SLP anomalies exist over the Arctic, and positive SLP anomalies are located over the North Atlantic, more like an NAO pattern (Fig. 5a). Similarly, the AO for La Niña years also exhibits an NAO-like seesaw structure (Fig. 5b). The high similarity in the AO spatial structure between ENSO warm and cold phases can also be seen in the 500 hPa geopotential height field (Figs. 5c, d). No significant circulation anomaly center is displayed in the North Pacific region. This suggests that the late winter AO spatial structure manifests as a regional NAO pattern both in the ENSO warm and cold phases.

5 Possible mechanisms for ENSO impacts on the AO pattern

Several previous studies pointed out that some other atmospheric variability may exert some impacts on the AO spatial structure by modulating the inter-basin teleconnectivity (e.g., Wallace and Thompson 2002; Honda et al. 2005; Shi and Nakamura 2014). Figure 6a displays the scatterplot of the Arctic and Pacific center indices during late winter. For normal years, a significant linear correlation (R = -0.41) is obtained between the Arctic and Pacific centers. However,



We in Fig. 7a display the ENSO teleconnection to the extratropical atmosphere in late winter based on the regressed SLP anomalies on the Niño3.4 index. The El Niño winters usually witness significantly negative SLP anomalies in the North Pacific region through the well-known PNA teleconnection pattern (Horel and Wallace 1981). Positive and negative SLP anomalies are also shown in the Arctic and western Atlantic regions, respectively, but with relatively weak amplitude. It is found that the ENSO-associated atmospheric teleconnection to the North Pacific region almost overlaps the Pacific center of the AO pattern. The linearly clustered dots and the high correlation coefficient (R = -0.69) between the Niño3.4 and Pacific center indices (Fig. 7b) indicate that about 50% of the SLP variance of the Pacific center can be explained by the ENSO variability. Contrastingly, there is no statistically significant linear relationship of the Niño 3.4 with Arctic center indices (R = 0.06, Fig. 7c). The dominance of ENSO in the SLP variability over the North Pacific and the weak control of ENSO in the SLP variability over the Arctic center leads to the weakened linear relationship of the Arctic with the Pacific centers during ENSO years (Fig. 6a), thus the absence of the late winter AO's significant Pacific center based on the EOF (Figs. 3b, d). During normal winters without the disturbance from the ENSO, the teleconnectivity between the two active centers (i.e., the North Pacific and Arctic centers) is remarkably strengthened with a significant linear relationship.

We next show regressed SLP anomalies on the early winter Niño3.4 index (Fig. 8a) to find out why ENSO does not have a similar effect on the early winter AO pattern. Compared with those in late winter, the SLP anomalies in early winter exhibit a very different pattern and have much weaker amplitude. In particular, almost no significant anomalies can be seen in the North Pacific region, suggesting that the ENSO plays a minor impact on the SLP variability over the Pacific center in early winter. It is further confirmed by the scatterplot between the early winter Niño3.4 and Pacific center indices (Fig. 8b). No statistically significant linear relationship is established between them (R = -0.18). Likewise, the early winter Niño3.4 and Arctic center indices are not significantly correlated (R = -0.09, Fig. 8c). Therefore, ENSO cannot change the teleconnectivity between the two centers in early winter, which leads to almost no difference in the AO spatial patterns between normal years and ENSO years (Fig. 4a, b). We also examine the respective effects of



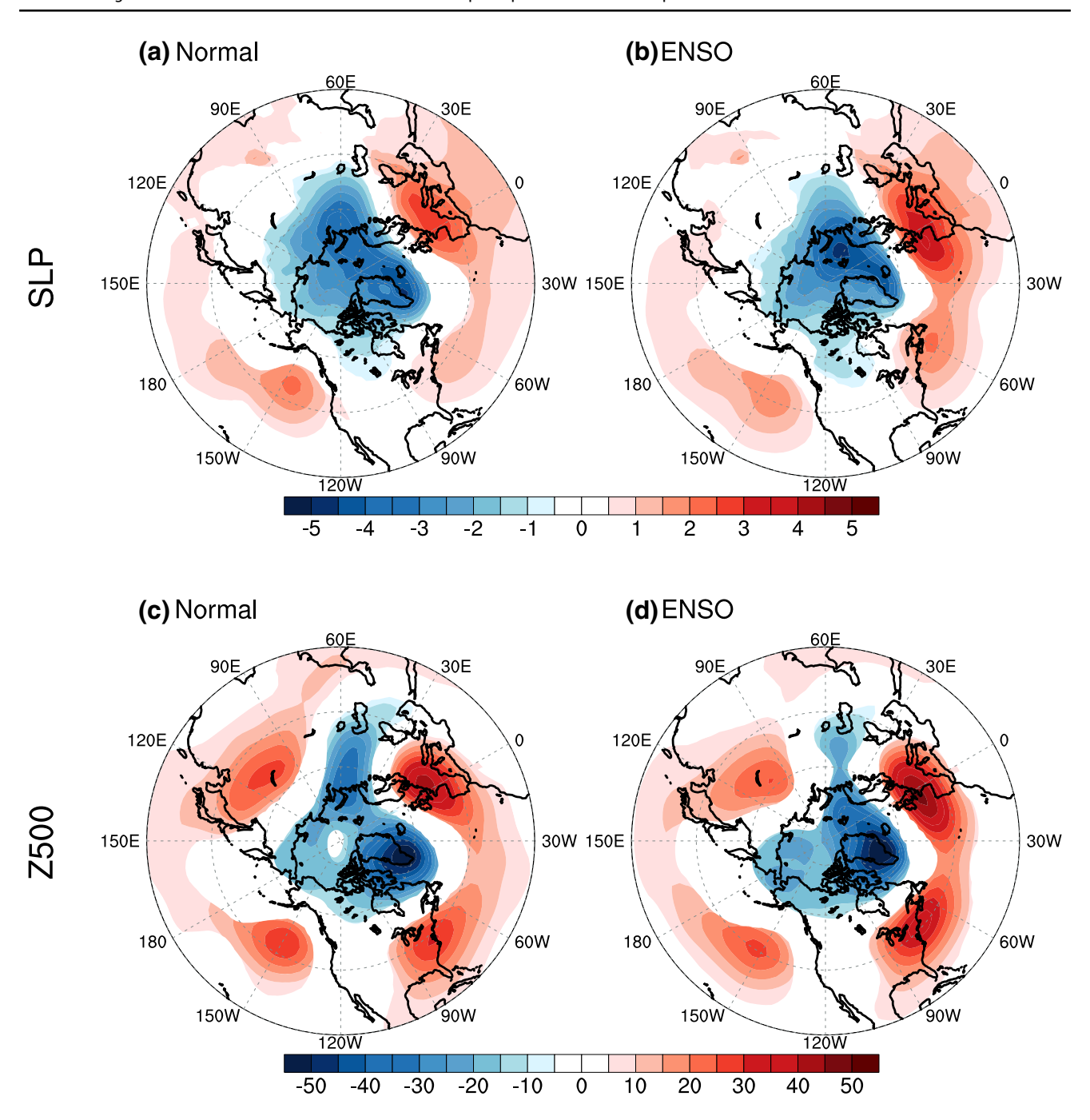
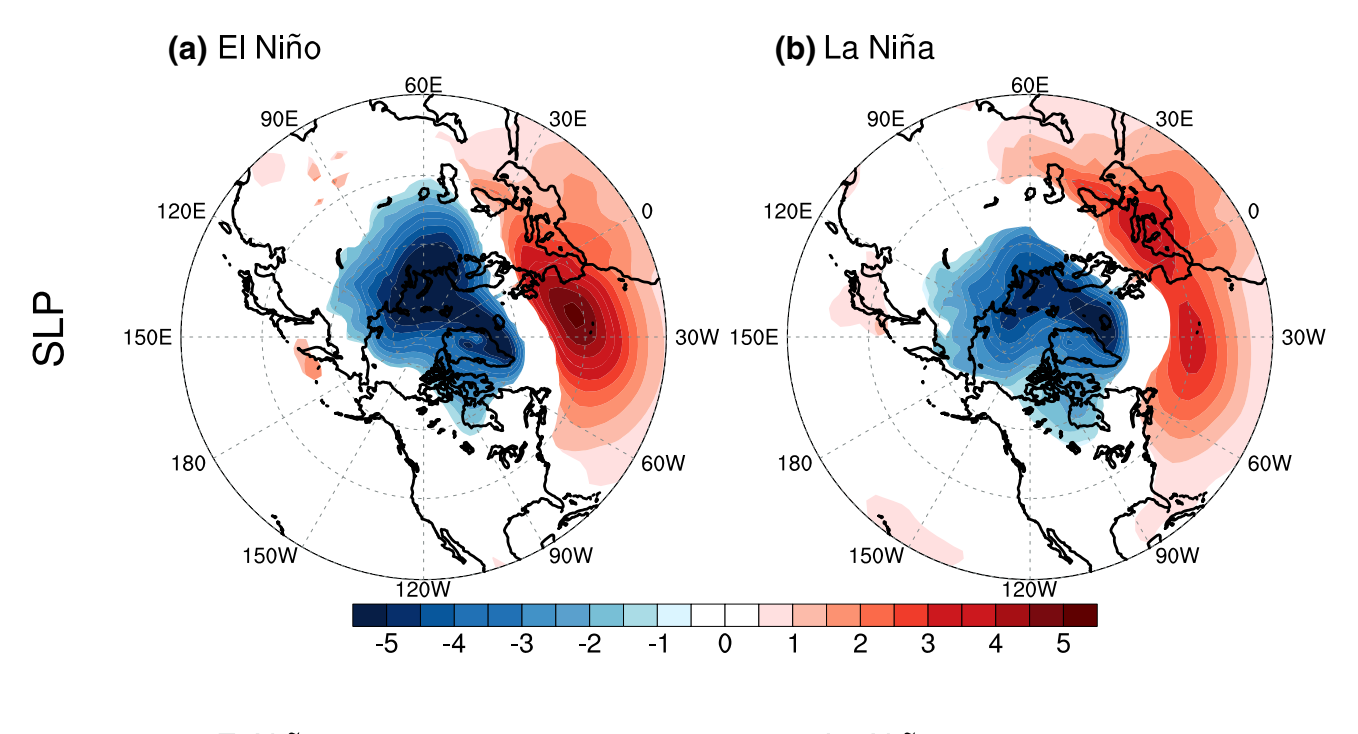


Fig. 4 Same as Fig. 3, but for the early winter

El Niño and La Niña on the SLP anomalies over the North Pacific and Arctic centers based on the composites shown in Fig. 9. For late winter, both El Niño and La Niña have significant effects on the SLP anomalies over the Pacific center while almost no response is detected over the Arctic center. In early winter, no obvious anomalies are detected over the North Pacific and Arctic centers both for El Niño and La Niña events. It has long been established that ENSO-associated tropical convection heating generates anomalous

upper-tropospheric divergence (convergence) in the tropics (subtropics), which further leads to anomalous vorticity forcing. This vorticity source is defined as the RWS by Sardeshmukh and Hoskins (1988), suggested as one of the main mechanisms responsible for the ENSO extratropical atmospheric teleconnection. We in Fig. 10 display the anomalous RWS associated with ENSO in early and late winter. In early winter, there exhibit weak positive RWS anomalies over the mid-latitude North Pacific (Fig. 10a), consistent with the





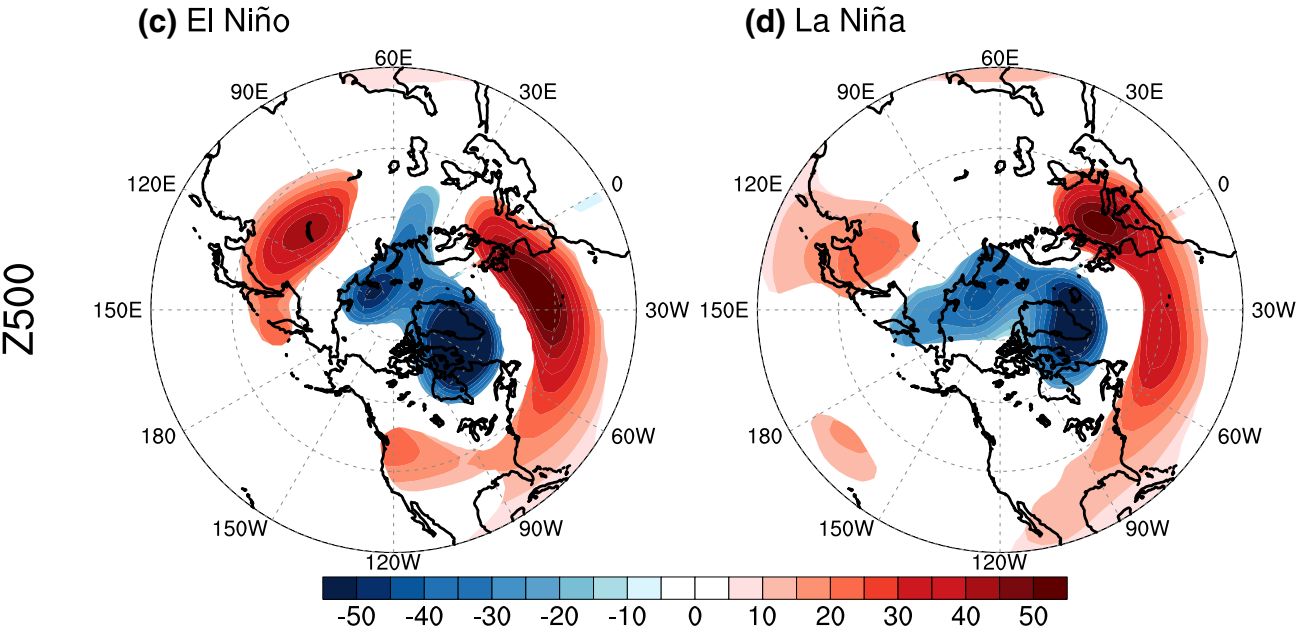


Fig. 5 a The late winter AO pattern for the El Niño years represented by the regressed anomalous pattern of SLP (hPa) on the late winter AO index during El Niño years of 1950–2019. **b** Same as **a**, but for

the La Niña years. ${\bf c}$ Same as ${\bf a}$, but for the Z500 anomalies (m). ${\bf d}$ Same as ${\bf b}$, but for the Z500 anomalies (m). Those anomalies significant above the 95% confidence levels are shaded

weak SLP response shown in Fig. 8a. Contrastingly, the ENSO-associated RWS anomalies are much stronger in late winter (Fig. 10b), corresponding to the remarkable enhancement of ENSO-associated SLP anomalies over the North Pacific (Fig. 7a). The dramatic sub-seasonal enhancement of the extratropical ENSO atmospheric response has also been addressed in previous research (Newman and Sardeshmukh 1998; Bladé et al. 2008; Kim et al. 2018). Bladé et al.

(2008) pointed out that there is a distinctive sub-seasonal and spatial shift in the sensitivity of the extratropical ENSO teleconnection. The tropical western Pacific SST anomalies contribute substantially to the early winter ENSO teleconnection while the tropical central Pacific forcing plays a prominent role in the late winter ENSO teleconnection. They further argued that this sensitivity shift is related to the sub-seasonal changes in the basic state and associated



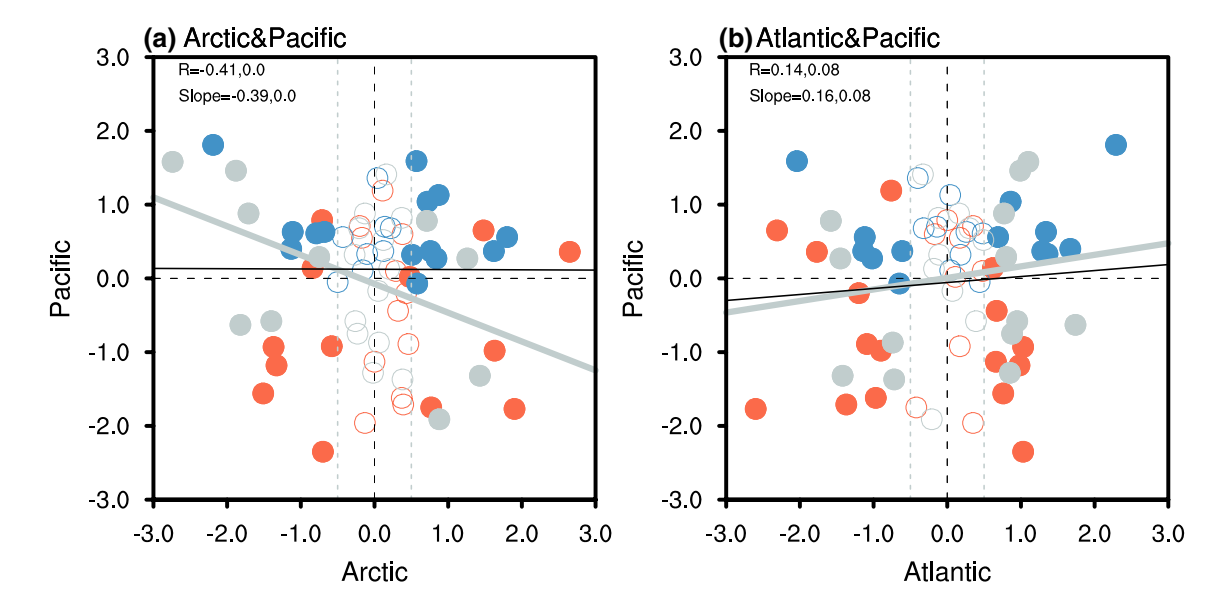


Fig. 6 a The scatter plot of the Arctic and Pacific center indices in late winter for the ENSO warm (red), cold (blue), and neutral (gray) events. The dots with the Arctic center index exceeding ± 0.5 standard deviation are marked as the filled circles. The linear fits for the normal years (gray line) and ENSO years (black line) are presented

with respective correlation coefficients (R) and slopes, and these fits are based on the filled circles. **b** Same as **a**, but for the Atlantic and Pacific center indices. The dots with the Atlantic center index exceeding ± 0.5 standard deviation is marked as the filled circles

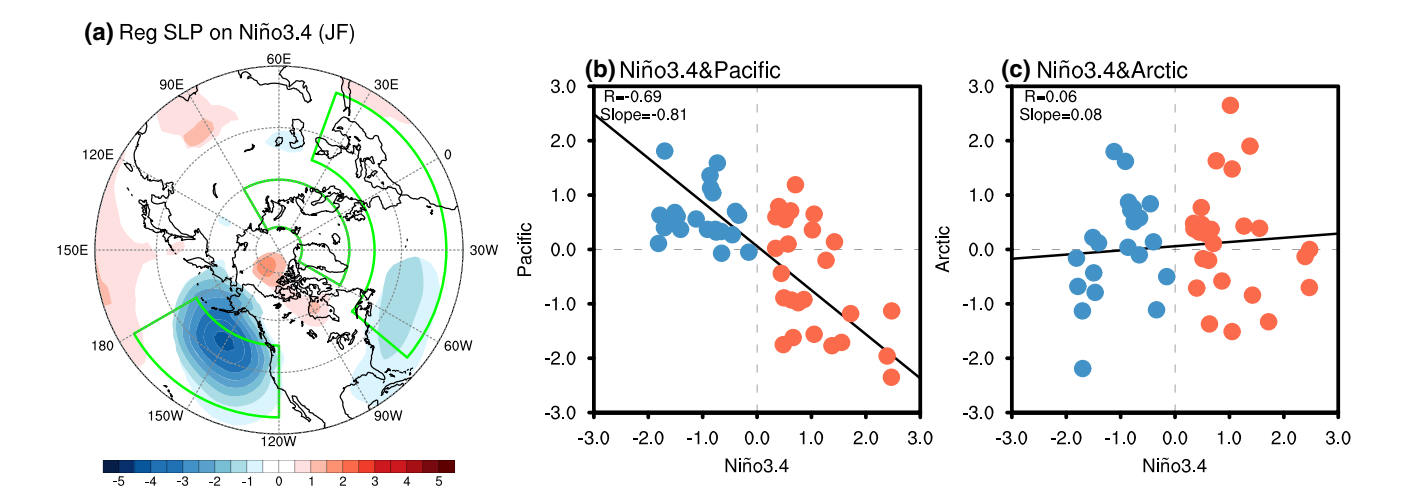


Fig. 7 a Regressed SLP anomalies (hPa) on the late winter Niño3.4 index. The anomalies significant above the 95% confidence levels are shaded. The green boxes in **a** are the domains used to define three action centers. **b** The scatter plot of the late winter Niño3.4 index and

Pacific center index for the ENSO warm (red) and cold (blue) events. The linear fit for the ENSO years (black line) is displayed with the correlation coefficient (R) and slope. **c** Same as **b**, but for the late winter Niño3.4 index and Arctic center index

Rossby waveguide (Newman and Sardeshmukh 1998). In addition to the change in the basic state, Kim et al. (2018) emphasized that the relative magnitude of these two tropical forcings is important in the sub-seasonal evolution of the ENSO teleconnection.

This observed modulation of the AO structure by ENSO is further substantiated by the modeling simulation. In the AMIP-style simulations of the MRI-ESM-2-0 model, the observed sub-seasonal enhancement in the extratropical

ENSO teleconnection from early to late winter is simulated well (Fig. 11). Correspondingly, the sub-seasonal variation in the AO spatial structure from early to late winter can be captured by this model. Consistent with the observation (Fig. 1a, b), the simulated AO-related SLP anomalies in early winter exhibit a high degree of annularity like an AO traditional pattern (Fig. 12a), and the simulated positive SLP anomalies over the North Pacific disappear in late winter despite that other two centers remain almost the



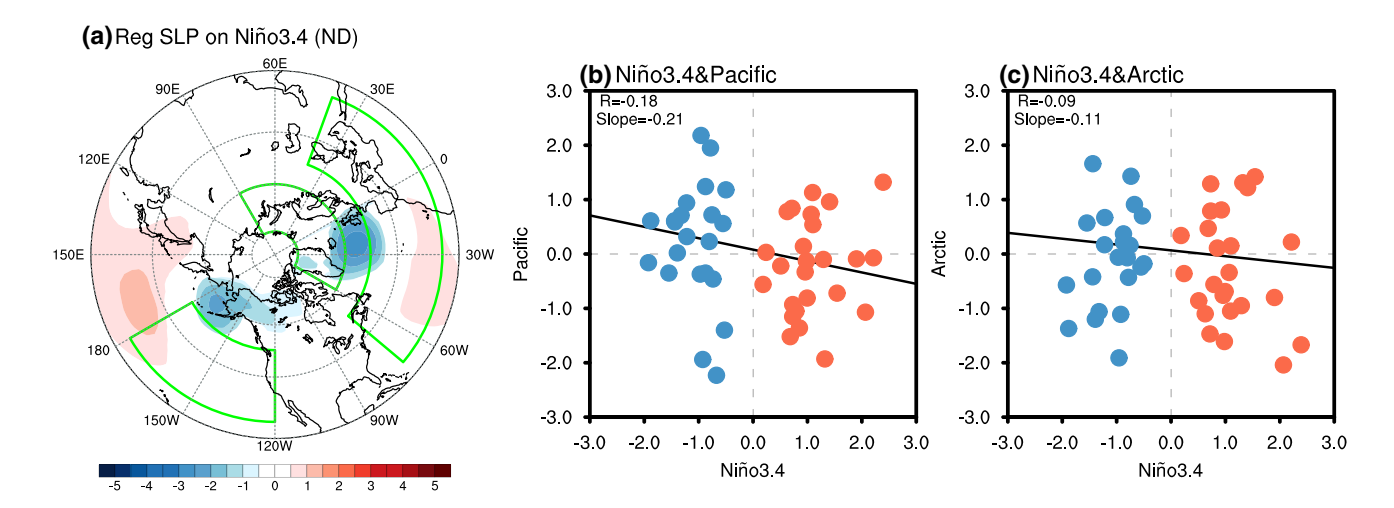
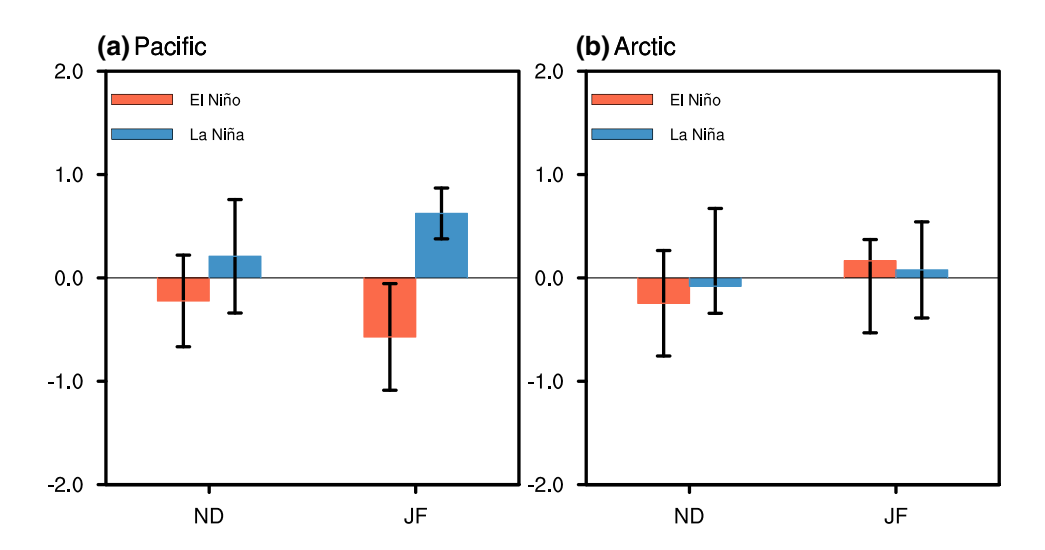


Fig. 8 Same as Fig. 7, but for the early winter

Fig. 9 a Composite Pacific center index anomalies for the El Niño (red bars) and La Niña (blue bars) events in early and late winter with error bars of one standard deviation. b Same as a, but for the Arctic center index



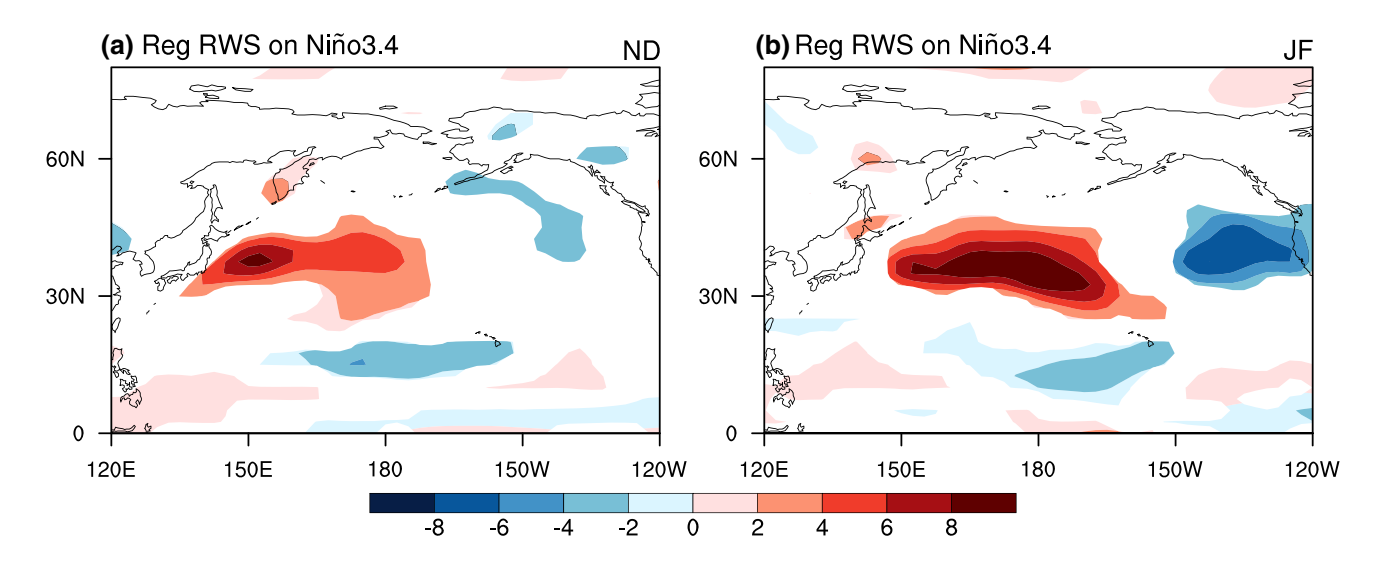


Fig. 10 a Regressed RWS anomalies $(10^{-11}S^{-2})$ at 200 hPa on the early winter Niño3.4 index. **b** Same as **a**, but for the late winter. The RWS anomalies significant above the 95% confidence levels are shaded



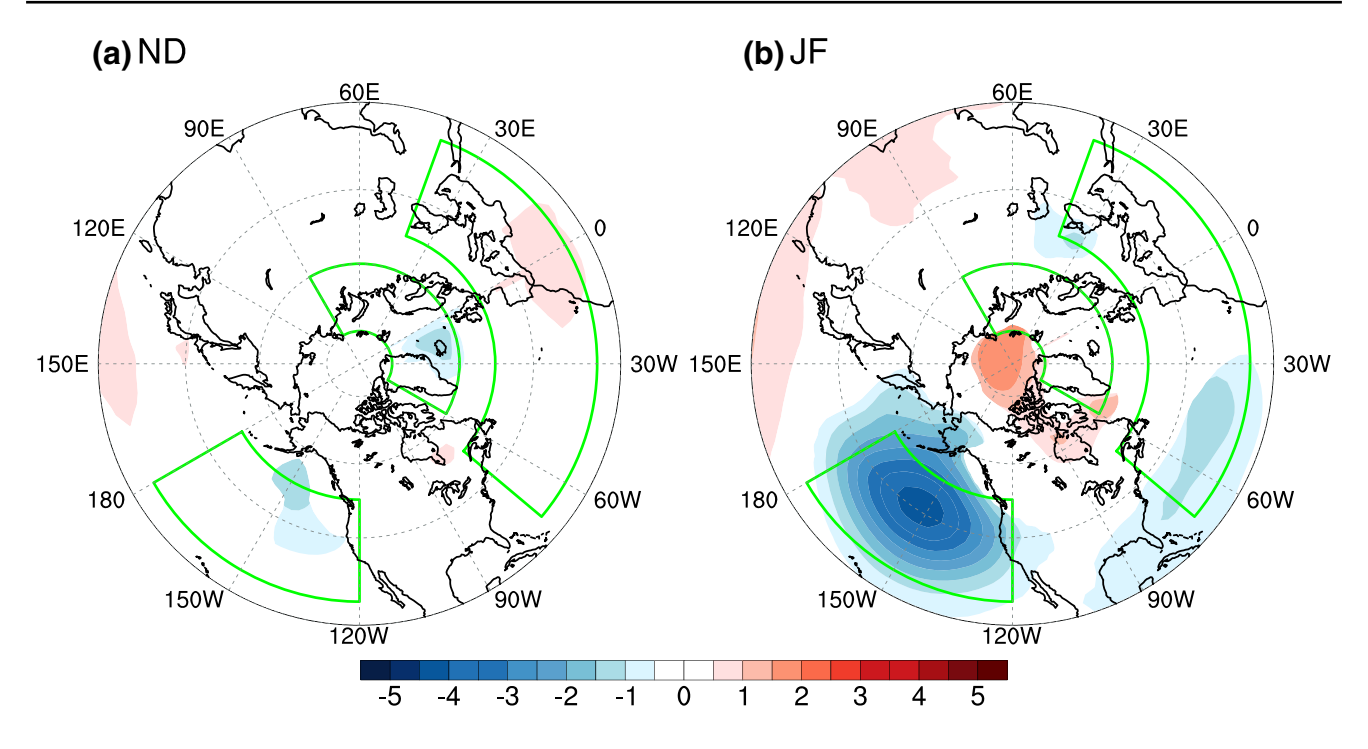


Fig. 11 a Regressed SLP anomalies (hPa) on the early winter Niño3.4 index in MRI-ESM-2–0 AMIP-style simulations. **b** Same as **a**, but for the late winter. The anomalies significant above the 95%

confidence levels are shaded. The green boxes in ${\bf a}$ and ${\bf b}$ are the domains used to define three action centers

same (Fig. 12b). The scatterplots of the simulated AO and its Pacific center for early and late winter are also shown in Fig. 12c and d, respectively. The AO is significantly correlated with its Pacific center both in normal (R=0.52) and ENSO years (R=0.57) during early winter. In contrast, the AO has a statistically significant correlation (R=0.49) with its Pacific center for normal years while no significant relationship (R=0.17) is detected for ENSO years in late winter, in accordance with the results of observations (Fig. 2b, c).

6 Conclusions and discussion

Obvious differences in the AO structure are detected over the North Pacific between early and late winter in 1950–2019. In early winter, a traditional AO annular structure can be observed with three centers of action, one of which is over the Arctic and the other two of opposite signs span the midlatitudes. In contrast, the AO pattern in late winter changes remarkably, resembling a regional NAO pattern with the absence of the North Pacific center. This sub-seasonal change in the AO spatial pattern can be largely attributed to the enhancement of ENSO atmospheric teleconnections to the Northern Hemisphere from early to late winter. ENSO affects the winter AO pattern by modulating the teleconnectivity between its Arctic and Pacific centers. In late winter, the ENSO-associated circulation anomalies weaken

the teleconnectivity between the Arctic and Pacific centers, resulting in the absence of the AO's significant Pacific center. Moreover, El Niño and La Niña exert similar impacts onto the AO spatial structure. However, for early winter, the ENSO-associated atmospheric anomalies exhibit a very different pattern with a much weaker amplitude, having no significant impact on the teleconnectivity between the two centers.

This work highlights the crucial role of ENSO in affecting the spatial structure of the AO by using the monthlymean data. Since AO is intrinsically a short timescale process (Feldstein 2000; Dai and Tan 2017), we also examine our results from an "AO event" perspective. Figure 13 displays the scatterplot of the AO index at the peak day of each AO event and the Pacific center index in early and late winter. As displayed in Fig. 13a, there are 47 and 94 AO events detected in early winter during normal and ENSO years, respectively. Among them, the AO indices of 36/47 (77%) events during normal years and 66/94 (70%) events during ENSO years have the same signs as the Pacific center indices (i.e., traditional AO events). In late winter, there are 46 and 109 AO events detected during normal and ENSO years, respectively. The AO indices of 35/46 (76%) events during normal years and 54/109 (50%) events during ENSO years have the same signs as the Pacific center indices (Fig. 13b). Cheng and Tan (2019) show that the AO pattern obtained by the EOF analysis is a statistic



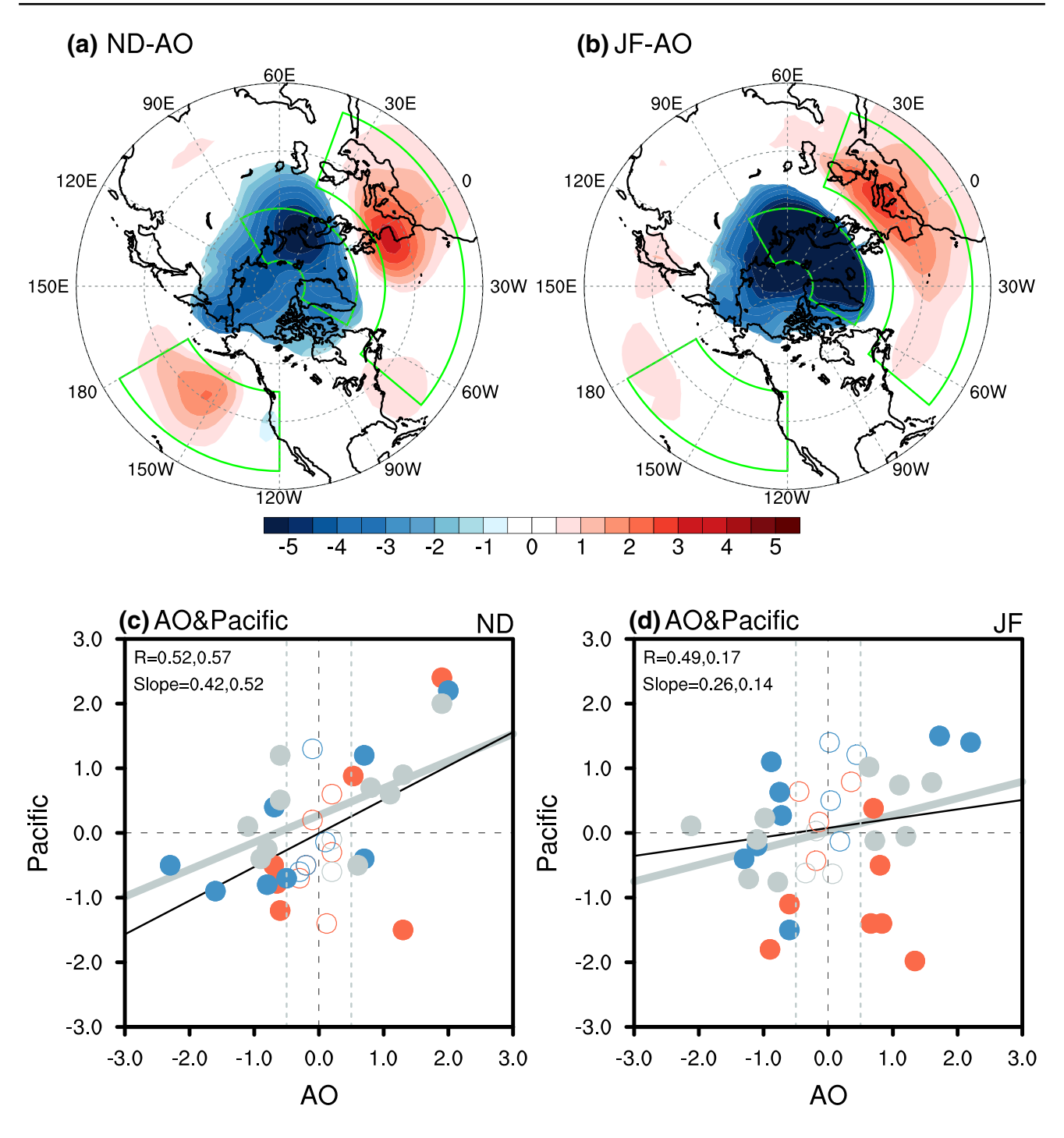


Fig. 12 a The early winter AO pattern represented by the regressed anomalous pattern of SLP (hPa) on the early winter AO index in MRI-ESM-2-0 AMIP-style simulations. **b** Same as **a**, but for the late winter. The anomalies significant above the 95% confidence levels are shaded. The green boxes in **a** and **b** are the domains used to define three action centers. **c** The scatter plot of the early winter AO index and Pacific center index for the El Niño (red), La Niña (blue),

and normal (gray) events in MRI-ESM-2-0 AMIP-style simulations. The dots with the AO index exceeding ± 0.5 standard deviation are marked as the filled circles. The linear fits for the normal years (gray line) and ENSO years (black line) are presented with respective correlation coefficients (R) and slopes, and these fits are based on the filled circles. **d** Same as **c**, but for the late winter

of two types of events—in-phase and out-of-phase AO events. For in-phase events, their Pacific and Arctic centers are of the same signs, while for out-of-phase events,

the two centers are of opposite signs (i.e., traditional AO events). We here show that the occurrence number of out-of-phase events during ENSO years in late winter decrease



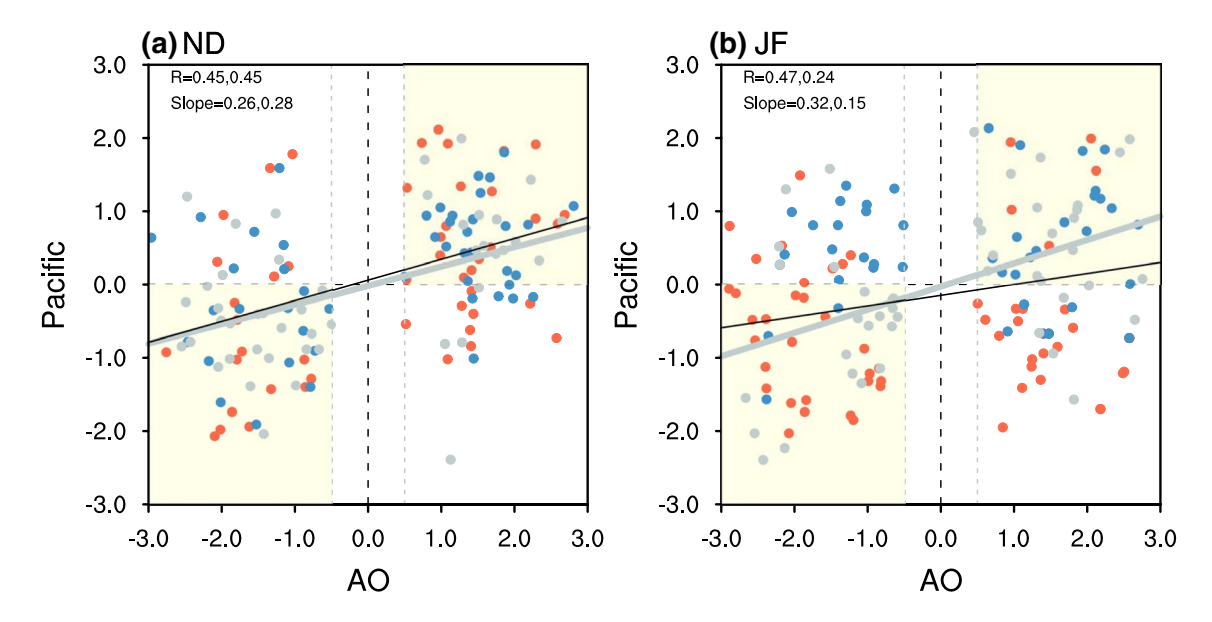


Fig. 13 a The Scatter plot of the early winter AO index at the peak day of each AO event and the Pacific center index for the El Niño (red), La Niña (blue), and normal (gray) years. The linear fits for normal years (gray line) and ENSO years (black line) are displayed

together with respective correlation coefficients (R) and slopes. **b** Same as **a**, but for the late winter. The yellow shading area denotes that the AO and its Pacific center indices are of the same signs

obviously in contrast to that in early winter $(70\% \rightarrow 50\%)$, which leads to the sub-seasonal change of the AO spatial pattern. It should be noted that ENSO can also alter the AO spatial structure via internal dynamics such as the modulation of basic flow and the stratospheric process (e.g., Lorenz and Hartmann 2003; Ineson and Scaife 2009; Smith and Kushner 2012). It deserves further study to fully understand the crucial role of ENSO in the AO spatial pattern. Most climate models have systematic biases in simulating the AO spatial pattern, the best-known of which is the discrepancy in the intensity of its Pacific center (e.g., Miller et al. 2006; Stoner et al. 2009; Gong et al. 2017). In most climate models, the magnitude of the Pacific center is generally over-estimated and even stronger than the Atlantic counterpart, possibly related to the inadequate description of the stratospheric processes in the models (Gong et al. 2019a). Nevertheless, there is at least one model that can realistically reproduce the sub-seasonal variation of the AO spatial structure due to ENSO-associated teleconnection to the extratropical atmosphere, providing a high potential for the improved seasonal prediction of the AO spatial structure and its related regional climate impacts.

Funding This work was funded by the National Nature Science Foundation of China (42125501 and 42088101).

Data availability The data that support the findings of this study are available from the following resources: https://psl.noaa.gov/data/gridded/data.ncep.reanalysis.html; https://psl.noaa.gov/data/gridded/tables/

daily.html; https://www.metoffice.gov.uk/hadobs/hadisst/data/download.html; https://esgf-node.llnl.gov/search/cmip6/.

Declarations

Conflict of interest The authors have no relevant financial or non-financial interests to disclose.

References

Ambaum MHP, Hoskins BJ, Stephenson DB (2001) Arctic oscillation or north atlantic oscillation? J Clim 14:13

Bjerknes JB (1967) Atmospheric teleconnections from the equatorial Pacific. Mon Weather Rev 97:163–172

Bladé I, Newman M, Alexander MA, Scott JD (2008) The late fall extratropical response to ENSO: sensitivity to coupling and convection in the tropical west Pacific. J Clim 21:6101–6118. https:// doi.org/10.1175/2008JCLI1612.1

Castanheira JM, Graf H-F (2003) North Pacific-North Atlantic relationships under stratospheric control? J Geophys Res Atmos. https://doi.org/10.1029/2002JD002754

Chen S, Yu B, Chen W (2014) An analysis on the physical process of the influence of AO on ENSO. Clim Dyn 42:973–989. https://doi.org/10.1007/s00382-012-1654-z

Chen S, Yu B, Chen W (2015) An interdecadal change in the influence of the spring Arctic Oscillation on the subsequent ENSO around the early 1970s. Clim Dyn 44:1109–1126. https://doi.org/10.1007/s00382-014-2152-2

Cheng Q, Tan B (2019) On the variation of the Pacific center: a revisit to the physical nature of Arctic Oscillation. Clim Dyn 53:1233–1243. https://doi.org/10.1007/s00382-018-4583-7

Choi K-S, Byun H-R (2010) Possible relationship between western North Pacific tropical cyclone activity and Arctic Oscillation. Theor Appl Climatol 100:261–274. https://doi.org/10.1007/s00704-009-0187-9



- Christiansen B (2002) On the physical nature of the Arctic Oscillation. Geophys Res Lett 29:52-1-52-4. https://doi.org/10.1029/2002G L015208
- Dai P, Tan B (2017) The nature of the Arctic Oscillation and diversity of the extreme surface weather anomalies it generates. J Clim 30:5563–5584. https://doi.org/10.1175/JCLI-D-16-0467.1
- Deser C (2000) On the teleconnectivity of the "Arctic Oscillation." Geophys Res Lett 27:779–782. https://doi.org/10.1029/1999G L010945
- Deser C, Simpson IR, Mckinnon KA, Phillips AS (2017) The northern hemisphere extratropical atmospheric circulation response to ENSO: how well do we know it and how do we evaluate models accordingly? J Clim 30:24
- Dommenget D, Latif M (2002) A cautionary note on the interpretation of EOFs. J Clim 15:10
- Eyring V, Bony S, Meehl GA et al (2016) Overview of the coupled model intercomparison project phase 6 (CMIP6) experimental design and organization. Geosci Model Dev 9:1937–1958. https://doi.org/10.5194/gmd-9-1937-2016
- Feldstein SB (2000) The timescale, power spectra, and climate noise properties of teleconnection patterns. J Clim 13:4430–4440. https://doi.org/10.1175/1520-0442(2000)013%3c4430:TTPSAC% 3e2.0.CO;2
- Feldstein SB, Franzke C (2006) Are the North Atlantic Oscillation and the northern annular mode distinguishable? J Atmos Sci 63:2915–2930. https://doi.org/10.1175/JAS3798.1
- Fisher RA (1915) Frequency distribution of the values of the correlation coefficient in samples from an indefinitely large population. Biometrika 10:507–521. https://doi.org/10.2307/2331838
- Fisher RA (1921) On the probable error of a coefficient of correlation deduced from a small sample. Metron 1:1–32
- Gong H, Wang L, Chen W et al (2017) Biases of the wintertime Arctic Oscillation in CMIP5 models. Environ Res Lett 12:014001. https://doi.org/10.1088/1748-9326/12/1/014001
- Gong H, Wang L, Chen W, Nath D (2018) Multidecadal fluctuation of the wintertime arctic oscillation pattern and its implication. J Clim 31:5595–5608. https://doi.org/10.1175/JCLI-D-17-0530.1
- Gong H, Wang L, Chen W et al (2019a) Diversity of the Wintertime Arctic Oscillation Pattern among CMIP5 Models: role of the Stratospheric Polar Vortex. J Clim 32:5235–5250. https://doi.org/ 10.1175/JCLI-D-18-0603.1
- Gong H, Wang L, Chen W (2019b) Multidecadal changes in the influence of the arctic oscillation on the east asian surface air temperature in boreal winter. Atmosphere 10:757. https://doi.org/10.3390/atmos10120757
- Honda M (2001) Interannual seesaw between the aleutian and icelandic lows. Part II: its significance in the interannual variability over the wintertime northern hemisphere. J Clim 14:19
- Honda M, Yamane S, Nakamura H (2005) Impacts of the aleutianicelandic low seesaw on surface climate during the twentieth century. J Clim 18:2793–2802. https://doi.org/10.1175/JCLI3419.1
- Horel JD, Wallace JM (1981) Planetary-scale atmospheric phenomena associated with the Southern Oscillation. Mon Weather Rev 109:813–829. https://doi.org/10.1175/1520-0493(1981)109% 3c0813:PSAPAW%3e2.0.CO;2
- Ineson S, Scaife AA (2009) The role of the stratosphere in the European climate response to El Niño. Nat Geosci 2:32–36. https://doi.org/10.1038/ngeo381
- Itoh H (2008) Reconsideration of the true versus apparent arctic oscillation. J Clim 21:2047–2062. https://doi.org/10.1175/2007JCLI21671
- Itoh H, Mori A, Yukimoto S (2007) Independent components in the northern hemisphere winter: is the arctic oscillation independent? J Meteorol Soc Jpn Ser II 85:825–846. https://doi.org/10.2151/ jmsj.85.825

- Kaiser HF (1958) The varimax criterion for analytic rotation in factor analysis. Psychometrika 23:187–200. https://doi.org/10.1007/BF02289233
- Kalnay E, Kanamitsu M, Kistler R et al (1996) The NCEP/NCAR 40-year reanalysis project. Bull Am Meteorol Soc 77:437–472. https://doi.org/10.1175/1520-0477(1996)077%3c0437:TNYRP% 3e2 0 CO:2
- Kim S, Son H-Y, Kug J-S (2018) Relative roles of equatorial central Pacific and western North Pacific precipitation anomalies in ENSO teleconnection over the North Pacific. Clim Dyn 51:4345–4355. https://doi.org/10.1007/s00382-017-3779-6
- Livezey RE, Mo KC (1987) Tropical-extratropical teleconnections during the northern hemisphere winter. Part II: relationships between monthly mean northern hemisphere circulation patterns and proxies for tropical convection. Mon Weather Rev 115:3115–3132. https://doi.org/10.1175/1520-0493(1987)115%3c3115:TET-DTN%3e2.0.CO;2
- Livezey RE, Masutani M, Leetmaa A et al (1997) Teleconnective response of the Pacific-North American region atmosphere to large central equatorial Pacific SST anomalies. J Clim 10:1787–1820. https://doi.org/10.1175/1520-0442(1997)010%3c1787: TROTPN%3e2.0.CO;2
- Lorenz DJ, Hartmann DL (2003) Eddy-Zonal flow feedback in the northern hemisphere winter. J Clim 16:1212–1227. https://doi. org/10.1175/1520-0442(2003)16%3c1212:EFFITN%3e2.0.CO;2
- Mao R, Gong D, Yang J, Bao J (2011) Linkage between the Arctic Oscillation and winter extreme precipitation over central-southern China. Clim Res 50:187–201. https://doi.org/10.3354/cr01041
- Miller RL, Schmidt GA, Shindell DT (2006) Forced annular variations in the 20th century Intergovernmental Panel on Climate Change Fourth Assessment Report models. J Geophys Res 111:D18101. https://doi.org/10.1029/2005JD006323
- Mori A, Kawasaki N, Yamazaki K et al (2006) A reexamination of the Northern Hemisphere Sea level pressure variability by the independent component analysis. SOLA 2:5–8. https://doi.org/10.2151/sola.2006-002
- Moron V, Gouirand I (2003) Seasonal modulation of the El Niñosouthern oscillation relationship with sea level pressure anomalies over the North Atlantic in October–March 1873–1996. Int J Climatol 23:143–155. https://doi.org/10.1002/joc.868
- Nakamura T, Tachibana Y, Honda M, Yamane S (2006) Influence of the Northern Hemisphere annular mode on ENSO by modulating westerly wind bursts. Geophys Res Lett 33:L07709. https://doi. org/10.1029/2005GL025432
- Neelin JD, Battisti DS, Hirst AC et al (1998) ENSO theory. J Geophys Res Oceans 103:14261–14290. https://doi.org/10.1029/97JC0 3424
- Newman M, Sardeshmukh PD (1998) The impact of the annual cycle on the North Pacific/North American response to remote low-frequency forcing. J Atmos Sci 55:1336–1353. https://doi.org/10.1175/1520-0469(1998)055%3c1336:TIOTAC%3e2.0.CO;2
- Philander SG (2018) El Niño, La Niña, and the Southern Oscillation. Princeton University Press
- Rayner NA, Parker DE, Horton EB et al (2003) Global analyses of sea surface temperature, sea ice, and night marine air temperature since the late nineteenth century. J Geophys Res Atmos. https:// doi.org/10.1029/2002JD002670
- Sardeshmukh PD, Hoskins BJ (1988) The generation of global rotational flow by steady idealized tropical divergence. J Atmos Sci 45:1228–1251. https://doi.org/10.1175/1520-0469(1988)045% 3c1228:TGOGRF%3e2.0.CO;2
- Shi N, Nakamura H (2014) Multi-decadal modulations in the Aleutian-Icelandic low seesaw and the axial symmetry of the Arctic Oscillation signature, as revealed in the 20th century reanalysis. Tellus Dyn Meteorol Oceanogr 66:22660. https://doi.org/10.3402/tellu sa.v66.22660



- Smith KL, Kushner PJ (2012) Linear interference and the initiation of extratropical stratosphere-troposphere interactions. J Geophys Res Atmos. https://doi.org/10.1029/2012JD017587
- Stoner AM, Hayhoe K, Wuebbles D (2009) Assessing general circulation model simulations of atmospheric teleconnection patterns. J Clim 22:4348–4372. https://doi.org/10.1175/2009JCL12577.1
- Thompson DWJ, Wallace JM (1998) The Arctic oscillation signature in the wintertime geopotential height and temperature fields. Geophys Res Lett 25:1297–1300. https://doi.org/10.1029/98GL00950
- Thompson DWJ, Wallace JM (2000) Annular modes in the extratropical circulation part I: month-to-month variability. J Clim 13:17
- Thompson DWJ, Wallace JM (2001) Regional climate impacts of the northern hemisphere annular mode. Sci New Ser 293:85–89
- Wallace JM, Thompson DWJ (2002) The Pacific Center of action of the northern hemisphere annular mode: real or artifact? J Clim 15:5
- Wang D (2005) Winter Northern Hemisphere surface air temperature variability associated with the Arctic Oscillation and North Atlantic Oscillation. Geophys Res Lett 32:L16706. https://doi.org/10. 1029/2005GL022952

- Wang H, Fu R (2000) Winter monthly mean atmospheric anomalies over the North Pacific and North America Associated with El Nino SSTs. J Clim 13:13
- Yukimoto S, Kawai H, Koshiro T et al (2019) The Meteorological Research Institute Earth System Model Version 2.0, MRI-ESM2.0: description and basic evaluation of the physical component. J Meteorol Soc Jpn 97:931–965. https://doi.org/10.2151/ jmsj.2019-051

Publisher's Note Springer Nature remains neutral with regard to jurisdictional claims in published maps and institutional affiliations.

Springer Nature or its licensor holds exclusive rights to this article under a publishing agreement with the author(s) or other rightsholder(s); author self-archiving of the accepted manuscript version of this article is solely governed by the terms of such publishing agreement and applicable law.

